Experimental study of combustion noise radiation during transient turbocharged diesel engine operation

Evangelos G. Giakoumis*, Athanasios M. Dimaratos and Constantine D. Rakopoulos

Internal Combustion Engines Laboratory, Department of Thermal Engineering, School of Mechanical Engineering, National Technical University of Athens
9 Heroon Polytechniou St., Zografou Campus, 15780 Athens, Greece

ABSTRACT

Diesel engine noise radiation has drawn increased attention in recent years since it is associated with the passengers' and pedestrians' discomfort, a fact that has been acknowledged by the manufacturers and the legislation in many countries. In the current study, experimental tests were conducted on a truck, turbocharged diesel engine in order to investigate the mechanism of combustion noise emission under various transient schedules experienced during daily driving conditions, namely acceleration and load increase. To this aim, a fully instrumented test bed was set up in order to capture the development of key engine and turbocharger variables during the transient events. Analytical diagrams are provided to explain the behavior of combustion noise radiation in conjunction with cylinder pressure (spectrum), turbocharger and governor/fuel pump response. Turbocharger lag was found to be the main cause for the noise spikes during all test cases examined, with the engine injection timing calibration and the slow adjustment of cylinder wall temperature to the new fueling conditions playing a vital role. The analysis was extended with a quasi-steady approximation of transient combustion noise using steady-state maps, in order to better highlight the effect of dynamic engine operation on combustion noise emissions.

Keywords: diesel engine; combustion noise; acceleration; load increase; turbocharger lag;

Classifications: 2.040 Diesel Engines; 2.070 Combustion

* Corresponding author. Tel.: +30 210 772 1360; fax: +30 210 772 1343.

E-mail address: vgiakms@central.ntua.gr (E.G.Giakoumis).

Nomenclature

p	pressure (bar)
φ	crank angle
A/C	aftercooler
BDC	bottom dead center
CA	crank angle
EGR	exhaust gas recirculation
FSO	full scale output
T/C	turbocharger
TDC	top dead center

1. Introduction

The turbocharged diesel engine is currently the preferred powertrain system in medium and medium-large unit applications (trucks, land traction, ship propulsion, electricity generation, etc). Moreover, it continuously increases its share in the highly competitive automotive sector, having already ensured a market share comparable to the one of the gasoline engine in the European Union. The most attractive feature of the diesel engine is its very good fuel efficiency, which can surpass a value of 40% in vehicular applications and even 50% in large, two-stroke units used for marine propulsion or electricity generation. Consequently, diesel-engined vehicles achieve much lower fuel consumption and reduced CO_2 emissions than their similarly rated spark ignition counterparts over the entire engine operating range and for their whole lifetime. From an acoustic point of view, however, the diesel engine remains by far inferior to the gasoline engine, being a very complex system comprising various dynamic forces acting on an equally complex structure of varying stiffness, damping and response characteristics.

The three primary sources of noise generation in a diesel engine are: gas-flow, mechanical processes, and combustion [1–3]. Gas-flow noise, usually low frequency controlled, is associated with the intake and exhaust processes, including turbocharging and the cooling fan. Mechanical noise comprises both rotating and reciprocating engine components contribution; it originates from inertia forces causing piston slap (impact of

piston on the cylinder wall, most notably when moving from TDC to BDC during expansion), from gears, tappets, valve trains, timing drives, fuel injection equipment and bearings.

The mechanism behind the third source of noise, namely combustion noise, lies in the (high) rate of cylinder pressure rise $dp/d\varphi$, mainly after the ignition delay period, which causes discontinuity in the cylinder pressure frequency spectrum and increase in the level of the high-frequency region, resulting in vibration of the engine block and, ultimately, in combustion noise radiation (the characteristic diesel combustion 'knock'). The combustion noise radiation manifests itself in the domain from a few hundred up to a few thousand Hz; on the other hand, the engine firing frequency is of the order of a few tens Hz. It should be pointed out that, although mechanical and gas-flow originated noise is encountered during gasoline engine operation too, problems associated with combustion are primarily restricted to diesel engines, with their spark ignition counterparts behaving noisy only when abnormal combustion (detonation) is experienced.

Combustion chamber design and injection parameters, e.g. timing, amount and rate of fuel injected during pre- and main injections, play a principal role in combustion noise emission by defining the exact rate of heat release during steady-state or transient conditions [4]. In order to analyze this source of noise, the cylinder pressure signal is usually examined on the frequency spectrum, for example using Fourier transform [1,5]; Russell and Haworth [6] and Pischinger et al. [7] discuss various methods for measuring and analyzing combustion noise.

Overall, engine noise measured 1 m away from the engine surface typically ranges from 80–110 dBA depending, mainly, on engine size, speed and injection system. Particularly for diesel-engined vehicles, the unpleasant combustion knock is also a matter of passengers and pedestrians discomfort; it is not surprising then that the European Union (directives 70/157/EEC and 96/20/EC [8]), Japan and the US have imposed regulations concerning noise emissions from vehicles and railroads.

Anderton and co-workers [e.g. 9] pioneered the diesel engine noise research by investigating the effect of various parameters on noise generated from diesel engines during steady-state conditions such as two vs. four-stroke operation, naturally aspirated vs. turbocharged, cylinder configuration etc. The fundamental conclusion reached was that turbocharging the diesel engine produces lower high-frequency (this ultimately results in a slightly lower level of combustion noise) but higher low-frequency excitations;

the same results are observed when the engine operates on the two-stroke rather than the four-stroke cycle. Recent studies on steady-state (combustion) noise emissions have focused on the effects of injection pressure, profile and rate. Electronically controlled, common rail injection systems that split the injection event into one pilot and one main injection can prove beneficial by facilitating the physical preparation of the air-fuel mixture, thus reducing premixed combustion and limiting (combustion) noise radiation [10–12]. On the other hand, the emergence of new promising diesel combustion technologies, such as low temperature combustion and PCCI (premixed charge compression ignition), are based on lower cycle temperatures, for example using very high EGR rates, in order to simultaneously limit soot and NO_x emissions [13]; these technologies are expected to have a detrimental effect on combustion noise owing to the higher portion of premixed combustion the lower cycle temperatures induce [14].

Combustion noise development during a speed or load increase transient differs to a large extent from the respective steady-state operation; this was the result reached by the surprisingly few studies carried out so far [15–18]. The fundamental aspect of transient conditions of a turbocharged engine lies in the operating discrepancies compared to the respective steady-state ones (i.e. operation at the same engine rotational speed and fuel pump rack position). During steady-state operation, engine speed and fueling and, consequently, all the other engine and turbocharger properties remain practically constant; under transient conditions, however, the engine speed changes continuously following the forced change in fueling. As a result, the available exhaust gas energy varies affecting turbine enthalpy drop and, through the turbocharger shaft torque balance, the boost pressure and the air supply to the engine cylinders are influenced. However, due to various dynamic, thermal (including cylinder wall temperature) and fluid delays in the system that mainly originate in the turbocharger moment of inertia, a phenomenon referred to as turbocharger lag, combustion air-supply is delayed compared to fueling, affecting unfavorably torque build-up as well as pollutant and noise emissions [4,19].

Head and Wake [16] were among the first to study the influence of accelerating rate on the noise emitted during speed increase of a naturally aspirated diesel engine. Their main finding was that combustion noise is generally higher during transients, typically of the order of 4–7 dBA, compared with the respective steady-state conditions. Their important argument was that this increase was mainly due to the lower cylinder wall temperature during the first cycles of the transient event. An increase of piston slap

generated noise during transients was also reported. Similar results were reached by Rust and Thien [17], who also extended the analysis to load acceptance transients, again for naturally aspirated diesel engine operation. Dhaenens et al. [18] is the only known reference to have focused on noise development during a *turbocharged* diesel engine acceleration; their investigation, using an anechoic chamber, revealed that transient overall engine noise exceeded steady-state levels by 5 dBA maximum (measured at 1 m distance from the engine surface), while it was also characterized by a broadband level increase combined with amplified resonance effects. The above transient discrepancies have been reported to be even more prominent during cold starting, where the much lower cylinder wall temperatures lead to even longer ignition delay periods, hence harsher premixed combustion and higher noise emissions [20].

The target of this study is to expand on the very limited experimental investigation of transient (combustion) noise radiation of turbocharged diesel engines, and shed more light into the relevant phenomena and underlying mechanisms. Since, as mentioned earlier, combustion noise prevails over other, mechanically originated, noise radiation, only this source of noise was included in the present investigation. To this aim, an extended set of experimental tests was conducted on a medium-duty, turbocharged and after-cooled, direct injection, truck diesel engine applying a modern combustion noise-meter for accurate cylinder pressure data analysis. An important aspect of the current investigation is that it focuses on both fundamental transient schedules encountered in the daily vehicle driving, i.e. acceleration (which was the main focus of the research) and load increase. By so doing it is believed that useful overall conclusions on transient combustion noise radiation can be deducted.

2. Description of the experimental installation

A general layout of the test bed installation, the instrumentation used and the data acquisition system is illustrated in Fig. 1. A brief description of the individual components is provided in the following subsections.

2.1 Engine under study

The engine used in this study is a Mercedes-Benz OM 366 LA, turbocharged and after-cooled, direct injection diesel engine. It is widely used to power mini-buses and

small/medium trucks; its basic technical data are given in Table 1. Two notable features of the engine are, on the one hand its retarded fuel injection timing in order to achieve low NO_x emissions (as will be discussed later in the text, this has a strong influence on combustion noise radiation too) and, on the other hand, the fuel-limiter (cut-off) function in order to limit the exhaust smoke level during demanding conditions such as transients or low-speed, high-load steady-state operation. The engine was coupled to a hydraulic dynamometer, which allows a good simulation of a vehicle's acceleration as will be explained later in the text. The fuel used in the experiments is typical automotive diesel oil with the following properties: density 837 kg/m^3, cetane number 50, and lower calorific value 42,700 kJ/kg.

2.2 Combustion noise measurement

Combustion noise measurement was achieved using the AVL 450 combustion noise-meter. Its operating principle is based on the analysis of the cylinder indicator diagrams on the frequency domain, applying a series of filters to it [21]. Initially, the cylinder pressure signal passes through a U-filter, corresponding to the frequency attenuation of the engine block. Afterwards, there is a possibility of filtering combustion chamber resonance with selectable low-pass filters, switchable on the front panel of the instrument, which, however, may induce measuring faults. Finally, the signal is guided through an A-filter that matches a standard value correction in acoustics to the audible characteristics of the human ear (dBA). The produced output signal is further processed by RMS (root mean square) conversion to logarithmic DC values that relate to the aural threshold. The final output signal is given as a digital display (in dBA) on the front panel of the instrument as well as an analogue voltage proportional to the combustion noise value. The former output is used during steady-state measurements, while the latter is selected during transient testing. The total error of the meter is less than ±1 dBA. In the current work, the combustion noise-meter was placed after the cylinder pressure signal amplifier, as shown in Fig. 1, and was operated without any low-pass filters.

2.3 Measurement of engine and turbocharger operating parameters

The various engine and turbocharger operating parameters measured and recorded continuously were: engine speed; cylinder pressure; fuel pump rack position; boost pressure and turbocharger speed. The location of each measuring device on the

experimental test bed installation is shown in Fig. 1. A custom made ‘stop’ with various adjustable positions, each one corresponding to a specific engine speed, was fitted on the (accelerator) pedal in order to ensure constant pedal position at the end of each acceleration test as well as repeatability of the accelerations.

2.4 Data acquisition and processing system

All the above mentioned signals from the measuring devices and instruments are fed to the input of the data acquisition module, which is a Keithley KUSB 3102 ADC card connected to a PC via USB interface. The specific card has a maximum sampling rate of 100 ksamples/s, with a 12-bit resolution for its 8 differential analogue inputs. Following the storage of the recorded measurements into files, the data were processed using an in-house developed computer code.

2.5 Error analysis

For the present experimental work, the error analysis consists of identifying the measuring error (accuracy) of each device implemented in the test bed installation. Table 2 provides the accuracy of the measurements of the engine and turbocharger operating parameters, as declared by each device manufacturer.

3. Experimental procedure

The first task of the test bed installation was the investigation of the steady-state performance and combustion noise characteristics of the examined engine. To this aim, an extended series of steady-state trials was conducted, covering the whole engine speed and load operating range. Between two consecutive measurements, a time interval was allowed in order for the engine to stabilize at the new conditions. The criterion used here was the stabilization of the exhaust gas temperature.

The main task of the experimental procedure was to study the engine combustion noise development during various transient schedules, namely acceleration and load change (increase). Since the engine tested is of the automotive/truck type, the main focus was on acceleration transients. For the experimental investigation, the engine was coupled to a hydraulic dynamometer, consequently during all acceleration cases the brake load (resistance) increased accordingly. This fact is actually desirable, because

this is the real case when a vehicle accelerates in real-world driving; the increase in engine/vehicle speed results in an increase of both tire rolling (varies with the engine speed) and aerodynamic resistance (varies with the square of the engine speed). The acceleration tests were performed for various combinations of initial engine rotational speeds and loads, mimicking vehicle real acceleration under different (vehicle) speed and gear; the details of all examined test cases are summarized in Table 3, with a more detailed description of each test provided in the respective results subsection.

4. Results and discussion

4.1 Steady-state results

Figure 2 illustrates the steady-state combustion noise map of the engine in hand. The important feature of the specific engine calibration is that with increase of the load, a decreasing trend in the combustion noise is noticed, with the peak observed roughly at 30–40% load for all rotational speeds. This trend is largely attributed to the injection strategy of the engine, which with increasing load shifts the injection timing closer to (or even after) the TDC in order to limit NO_x emissions. Consequently, combustion starts later in the cycle in a more favorable air-environment, decreasing the ignition delay (identified in the cylinder pressure diagrams in Fig. 3 for two typical engine loads), and so the in-cylinder pressure gradient decreases too [22]. As a result, the radiation of combustion noise is noticeably limited, most particularly in the important high frequency spectrum (close and above 1 kHz), which is mainly representative of combustion excitation forces. In general, there are three features of the combustion process that can be identified by the pressure spectrum: the peak cylinder pressure is indicated by the pressure level at the low frequencies (e.g. 10–30 Hz); the mean rate of pressure rise is generally reflected in the 1–4 kHz region, whereas the high frequencies (>5 kHz) are usually indicative of pressure rise change rates at the actual start of combustion [1].

The above-mentioned decrease in the combustion noise radiation is demonstrated in Fig. 4 for the two loads of Fig. 3. For example, when the engine operates at 1800 rpm, a decrease of the order of 11 dBA (from 107 to 96 dBA) is experienced when moving from 30 to 80% load. As will be discussed later in the text, this injection calibration influences strongly the whole pattern of combustion noise during transients too.

It should be pointed out, however, that although the pressure derivative noise term decreases as the load increases, the fact that this term reaches its highest value after TDC, during the expansion stroke, means that most probably the total amount of 'in-cylinder'-borne noise (comprising both the combustion and mechanical contribution) might actually be higher, as it is a few degrees after the TDC that the highest values of piston slap are also experienced [1,2].

4.2 Acceleration tests results

4.2.1 Tests No. 1 and 2 – Acceleration from low initial load

Figure 5 illustrates the results for the first two acceleration tests (No. 1 and No. 2 in Table 3) commencing from the same initial operating conditions, i.e., engine speed 1035 rpm and 10% load. This test represents vehicle acceleration from idling conditions, when the first gear is selected in the gearbox. It is the final engine speed that varies between the two cases, with the brake loading following accordingly (since the brake connected to the engine is a hydraulic one, its torque rises with the second power of speed – the same applies for the aerodynamic resistance term for vehicular applications). The response of five engine and turbocharger operating parameters as well as the development of noise emission is demonstrated in this figure. These two tests are particularly demanding for both the engine and the turbocharger, since the latter accelerates from practically zero boost.

As is made obvious from Fig. 5, the fuel pump rack (identical profile with the amount of injected fuel quantity) responds almost instantly to the fueling increase command and shifts to its maximum position, leading to higher fueling. Particularly during the most demanding test No. 2 (solid line), the fuel pump rack responds in two stages (lasting for 12 engine cycles or 1.17 s); initially, a rapid shift to a first peak position is observed, followed by a 'smoother' movement to the maximum position. The latter behavior highlights in the most explicit way the fuel limiter operating principle that does not allow sharp fueling increases when the boost pressure is still low. Indeed, boost pressure remains practically unchanged during the early transient cycles (middle-right sub-diagram of Fig. 5). Clearly, the increased exhaust gas power is not capable of instantly increasing the turbine power output, largely owing to the turbocharger inertia, so that the compressor operating point moves rather slowly towards the direction of increased boost pressure and air-mass flow-rate; during this period, known as

turbocharger lag, the engine is practically running in naturally aspirated mode or with very low boost [3,19].

Not surprisingly, the above-mentioned engine response pattern influences decisively the emission of combustion noise too (upper-right sub-diagram of Fig. 5). The main mechanism behind the increase in combustion noise radiation during transients lies in the operating principles of a transient event. In the first cycles after a speed increase, such as the ones demonstrated in Fig. 5, the injected fuel quantity has already increased substantially cooling down the charge-air temperature; however, the cylinder wall temperature is still low (up to 100°C lower than the corresponding steady-state conditions [17]), as the thermal transient proceeds at a much slower rate due to the, generally, high cylinder wall thermal inertia [23]. Moreover, the rapid increase in fuel injection pressure upon the onset of each instantaneous transient cause the penetration of the liquid fuel jet within the combustion chamber to increase. Since the initial higher-pressure fuel jets are injected into an air environment that is practically unchanged from the previous steady-state conditions, the higher-momentum fuel jet is not accompanied by equally enhanced gas motion. Thus, liquid fuel impingement on the still cool combustion walls increases, lowering the rate of mixture preparation [24]. The combination of increased fueling with the 'cooled' charge-air temperatures deteriorate the mixture preparation process, resulting in longer ignition delay, hence more intense premixed combustion periods with faster, more abrupt heat release; the latter manifests itself as steeper cylinder pressure gradients $dp/d\varphi$ and, consequently, higher combustion noise levels, as demonstrated in the upper-right sub-diagram of Fig. 5.

Particularly during test No. 2, the above-mentioned mismatch between fueling, air-supply and cylinder wall temperature is even more prominent (it lasts longer too) owing to the higher demanded speed (steeper accelerator pedal push), which leads to higher initial fueling change, hence harder acceleration schedule compared with test No. 1; consequently, more elevated combustion noise values are experienced (up to 4 dBA compared with test No. 1).

In order to shed more light into the impact of transient conditions on the combustion noise radiation, a quasi-steady prediction has been also undertaken (for the instantaneous rotational speed and fuel pump rack position of each cycle during the transient event). Initially, steady-state maps of all interesting engine operating parameters were constructed with respect to engine speed and fuel pump rack position, based on the detailed steady-state measurements. Afterwards, the time (or engine

cycle) histories of engine speed and fuel pump rack position were fed as inputs to the look-up tables, generating the quasi-steady values of noise emission and performance parameters. This means that the quasi-steady approximation provides an estimation of noise values if the engine was allowed to stabilize at each intermediate point of the transient event.

A typical example of quasi-steady approximation and its deviation from 'real' transient data is illustrated in Fig. 6. Here, test case No. 1 is studied on a quasi-steady basis and compared with the experimental transient measurements. The development profiles of engine speed, rack position, boost pressure and combustion noise radiation are presented. The major observations concern on the one hand the absolute values of (peak) noise emissions, and on the other hand the timing at which these occur.

Combustion noise radiation becomes higher during the transient event (especially during the turbocharger lag cycles) compared with the quasi-steady operation, confirming the results of previous research [18] as regards both absolute difference value and development profile; the difference is of the order of approximately 3 dBA for the rather moderate speed increase of Test No. 1. Moreover, the peak noise value occurs somewhat earlier during the transient event. The three basic reasons that explain these discrepancies between quasi-steady and experimental transient noise values are summarized below:

1. The air-mass flow-rate develops during the transient event at a much different (slower) rate owing to turbocharger lag (greater differences the higher the acceleration or the faster the accelerator pedal change); the boost pressure development in Fig. 6 highlights explicitly this behavior.
2. Fuel delivery to the cylinders differentiates too, owing to the injection timing alteration during transients; the developing value of residual pressure in the fuel injection line [4] and the instantaneous torsional deformations in the driving system of the (mechanical) fuel injection pump cause rapid and considerable changes to the dynamic injection, needle lift and, ultimately, fueling rate [25].
3. Cylinder wall temperature develops much slower during acceleration, owing to the thermal inertia of the cylinder wall - coolant system. Lubrication oil temperature, which plays an important role too through its impact on engine friction, develops much slower during transients compared with steady-state conditions [26].

The above statements are highlighted in Figs 7 and 8 that demonstrate the cylinder pressures and cylinder pressure levels for the two cycles exhibiting the higher noise

difference between the two examined cases (real transient measurement and quasi-steady approximation). Clearly, a more abrupt premixed combustion phase is experienced during the transient event (identified in the steeper cylinder pressure increase after the ignition delay period in Fig. 7) that also transforms into higher pressure level, practically for the whole spectrum above 200 Hz (Fig. 8).

4.2.2 Tests No. 3 and 4 – Acceleration from low or high initial load

Figure 9 investigates the effect of initial loading on the engine acceleration profile. Here, two tests were performed (almost identical in terms of engine speed increase), differing only as regards the initial engine loading. One low and one medium initial load were tried, with the final load affected accordingly following the response of the hydraulic brake; the rate of the pedal change was maintained the same for both cases. The two selected loads represent the gear engaged, with the low load corresponding to first gear and the medium load to fourth gear in the gearbox of a truck or bus.

One of the most influential parameters in the results of Fig. 9 is the initial turbocharger operating point, which affects accordingly the development of all interesting variables [27] and most remarkably the development of combustion noise. Unlike the previous tests No. 1 and 2, combustion noise shows a decreasing trend for the case of acceleration test No. 4 (the one commencing from the medium load and resulting in a high final load). This finding confirms the results of previous research [11], although it seems to contradict the intuition that increasing loading (during the transient event) might lead to higher noise emissions.

The trend observed in Fig. 9 for the noise development of Test No. 4 (solid line) implies that a reduced rate of cylinder pressure rise (i.e., decreasing 1^{st} derivative of cylinder pressure) throughout the transient event is encountered; this may be further ‘assisted’ by injection timing retard and shorter ignition delay period. Indeed, these remarks are true for the engine in hand, and can be documented with reference to Fig. 10, where the indicator diagrams for two intermediate cycles of acceleration tests No. 3 and 4 are presented together with their respective 1^{st} derivative graphs.

The underlying principle for the behavior noticed in Figs 9 and 10 is that, as the acceleration develops and engine speed (and, mainly, loading) increases, the fuel is injected later in the compression stroke, in an environment of higher pressure and temperature resulting in faster ignition. Recall from the steady-state map of Fig. 2 that

the injection strategy of the particular engine is exactly this, i.e. later injection with increasing load for NO_x emission control. Consequently, there is a shorter premixed combustion phase at the 41st cycle compared with the 15th, resulting in a lower rate of cylinder pressure increase. In addition, during the 41st cycle of the medium-high loading acceleration case No. 4, the start of combustion has shifted after the 'hot' TDC (lower-right sub-diagram of Fig. 10), assisting further the decrease of the pressure increase rate. Thus, combustion noise decreases during the medium-high loading acceleration as the upper sub-diagram of Fig. 10 clearly demonstrates in the form of the decisive maximum cylinder pressure gradient. It should be pointed out however that this particular feature of the current engine does not necessarily apply to engines with exhaust gas recirculation, or to earlier engines without NO_x emission control.

4.2.3 Tests No. 5 and 6 – Slow and fast acceleration

A further important parameter that significantly affects engine and turbocharger response as well as noise emission development during acceleration is the rate of the (accelerator) pedal movement from the initial to its final position [3,26]; in real-world driving, this represents the driver aggressiveness. Its impact on engine performance and emissions is studied in Fig. 11. Here, an acceleration test from 1420 to 1845 rpm was performed twice, once in 'fast' and the second in 'slow' mode. The time needed for the fuel pump rack (i.e. amount of injected fuel) to shift to its maximum position can be used as an index of the time over which the pedal position change took place. This time was 1s for the 'fast' mode (which is actually the usual case in most real-world driving cases) and 5s for the 'slow' mode, with the latter representing a theoretical slow acceleration scenario.

From Fig. 11 it is made obvious that the difference in the acceleration rate on the combustion noise development can be quite important (up to 2.1 dBA), and the qualitative remarks that follow may be applicable on a general basis. The most important difference between the two acceleration modes is observed in the fuel pump rack position development. In the case of the rapid pedal push, the rack is forced to travel almost instantaneously to its maximum position before gradually settling down to its final steady-state value, corresponding to the desired engine speed. Again, the fuel pump rack responds in two stages; initially a rapid shift to a first peak position is observed, followed by a smoother movement to the maximum position. On the contrary, when the

pedal is pushed slowly (‘slow’ transient), the rack shifts at a much smoother rate (no fuel limiter action needed here), causing lower acceleration rates and slowing down the whole transient event, as is further documented in the maximum cylinder pressure response (upper-left sub-diagram of Fig. 11).

As regards the combustion noise radiation, and as was perhaps intuitively expected, only the development profile seems to be affected by the acceleration rate and not the maximum final values. The main finding is that noise emission develops in a smoother way too during the slow acceleration compared with the faster test (solid line); during the latter, noise peaks from the 75^{th} cycle, and remains at this value for the whole transient event, following closely the maximum cylinder pressure profile. The smother development of noise increase during the slow test lies in the corresponding slow fueling increase, which limited the transient discrepancies discussed in Section 4.2.1 and resulted ultimately in decreased $dp/d\varphi$ values.

4.3 Load increase tests results

The second class of transient operation investigated is the load increase transient event (test No. 7 in Table 3), the results of which are shown in Fig. 12. In general, although automotive engines do encounter load increase transients, for example when a vehicle climbs a hill, or when engaging the clutch after a gear change, these are not so pronounced as the ones experienced by industrial or marine engines. The most influential factor that determines the engine speed response here is the governor operating curves. Due to the much less tight governing of automotive engines compared with industrial ones, severe load changes on an uncontrolled automotive engine test bench may lead to engine stall. As a result, for the case demonstrated in Fig. 12, a rather slow movement of the brake control lever towards the direction of increased loading was chosen. Initially, the engine was operating at a high rotational speed and low load (10%); the new higher load was applied by shifting the brake lever position without changing the engine accelerator pedal position. This caused a large engine speed decrease (of the order of 800 rpm), which was decisive for the whole system response and combustion noise development.

The various parameters’ response during the load increase of Fig. 12 can be divided into three stages:

1) During the application of the new higher loading (this lasted for several (8) seconds, otherwise the engine would stall), the fuel pump governor responded by shifting the rack to a greater fuel delivery position based on the instantaneous speed drop. Following the increase in the applied loading, the engine speed fell at a rather moderate rate (this lasted for approximately 60 cycles). During this period, the turbocharger accelerated only moderately due to the small increase of the exhaust gas energy from the engine originating in the slow rack movement. A slight increase in the combustion noise radiation was also encountered owing to the fact that relatively larger amounts of fuel were injected into an air environment practically unchanged from the previous steady-state conditions. The increased fueling cooled down the air-supply, whereas the wall temperature could not instantly follow the increase in loading, hence a slightly more prolonged ignition delay was experienced, which in turn enhanced the premixed combustion phase and the radiated noise (see also Fig. 13, where selected cylinder pressure diagrams of each stage, together with the respective 1^{st} derivatives of the cylinder pressure are demonstrated).
2) During the second part, the engine speed decreased sharply; the rack managed to achieve an adequately high fuel delivery, thereby increasing the engine loading, so that the turbocharger accelerated quickly, and the boost pressure increased accordingly. At the same time, the wall temperature started to increase gradually according to the new loading conditions, and combustion noise radiation decreased sharply, namely from 108 to 100 dBA. The primary mechanism for the combustion noise behavior noticed during the second phase of the load increase in Fig. 12 is, largely, based on the steady-state noise map of Fig. 2. The engine injection strategy dictates later injection timings with increasing load for reduced NO_x emission, hence there is a) a shorter premixed combustion phase, as the fuel is injected later into a more favorable environment resulting in faster ignition, and b) the start of combustion is gradually shifted after the ‘hot’ TDC, as the right sub-diagram of Fig. 13 clearly shows. Both factors, assisted by the decrease of the engine speed, which also delays the injection timing, result in a much lower rate of cylinder pressure increase (left sub-diagram of Fig. 13), which ultimately led to lower combustion noise emissions. As is further documented in Fig. 14, which provides the corresponding cylinder pressure spectrum graphs for three selected cycles (No. 20 of stage 1, No. 110

of stage 2 and No. 180 of stage 3) of the transient test, the amplitude of the pressure level during cycle No. 110 of the second stage is lower than its counterpart of cycle No. 20 of the first stage, practically for the whole frequency spectrum. Confirming the results of previous research [28,29], as the premixed combustion is restrained (from cycle 20 to 110 and then to 180), the high frequency (above 500 Hz) components of the cylinder pressure level are also reduced, lowering also the amount of the radiated noise.

3) Finally, the third stage can be classified as the stabilization phase, with the engine speed, fuel pump rack, turbocharger properties, as well as the combustion noise stabilizing to their final steady-state values; the cylinder wall (not shown) followed too at a much slower rate. Largely owing to the increase of the cylinder wall temperature, which gradually adjusts to the new, increased fueling conditions, the ignition delay period is shortened additionally (right sub-diagram of Fig. 13), and the noise radiation during this stage becomes even lower, as the spectrum diagram of Fig. 14 further demonstrates (cycle 180).

Of course, owing to the turbocharger lag and the various internal ‘delays’ of each individual engine ‘sub-system’, the exact duration and the limits of each stage do not coincide for every variable examined, but rather there is a delay between the minima or maxima for each interesting property in Fig. 12.

5. Summary and conclusions

A fully instrumented test bed installation was developed in order to study the transient performance and combustion noise emissions of a truck, turbocharged diesel engine. A fast response combustion noise-meter was employed for measuring combustion noise radiation during a variety of acceleration and load increase tests experienced during daily driving conditions. The basic conclusions derived from the current investigation and for the specific engine-hydraulic brake configuration are:

1. As expected, turbocharger lag was found to be the most notable contributor for all transient test cases examined, and one of the major causes for the behavior of combustion noise radiation.
2. Confirming the results of previous research, the turbocharged diesel engine was found to behave noisier at acceleration compared with the steady-state operation (up to almost 3 dBA for the case examined in this work), and this was attributed,

further to the turbocharger lag effect, to the slow adjustment of the cylinder wall temperature to the increased fueling demands.

3. Fuel limiter action, governing, turbocharger initial operating point and, particularly, the engine injection timing calibration were found to play a decisive role on the emission of combustion noise by determining the cylinder pressure gradient and frequency spectrum; they also influenced the engine speed and turbocharger response.
4. Transient noise radiation was smoothed the slower the acceleration, the higher the initial operating (turbocharger) point, and the smaller the demanded speed increase.
5. Load increases of an automotive engine on an uncontrolled test bench are strongly influenced by the 'loose' governing, leading to considerable speed drops affecting accordingly the whole system response and combustion noise development.

References

[1] Lilly LRC. Diesel engine reference book. London: Butterworths; 1984.

[2] Taylor CF. The internal combustion engine in theory and practice, vol. 2. Cambridge, MA: MIT Press; 1985.

[3] Li W, Gu F, Ball AD, Leung AYT, Philipps CE. A study of the noise from diesel engines using the independent component analysis. Mechanical Systems and Signal Processing 2001;15:1165-84.

[4] Rakopoulos CD, Giakoumis EG. Diesel engine transient operation. London: Springer; 2009.

[5] Austen AEW, Priede T. Origins of diesel engine noise. Institution of Mechanical Engineers, symposium on 'engine noise and noise suppression', 1958, pp. 19–32.

[6] Russell MF, Haworth R. Combustion noise from high speed direct injection diesel engines. SAE paper no. 850973, 1985.

[7] Pischinger FF, Schmillen KP, Leipold FW. A new measuring method for the direct determination of diesel engine combustion noise. SAE paper no. 790267, 1979.

[8] Commission Directive 96/20/EC of 27 March 1996 adapting to technical progress Council Directive 70/157/EEC relating to the permissible sound level and the exhaust system of motor vehicles.

[9] Anderton D, Baker J. Influence of operating cycle on noise of diesel engines. SAE paper no. 730241, 1973.

[10] Carlucci P, Ficarrela A, Laforgia D. Study of the influence of the injection parameters on combustion noise in a common-rail diesel engine using anova and neural networks. SAE paper no. 2001-01-2011, 2001.

[11] Kondo M, Kimura S, Hirano I, Uraki Y, Maeda R. Development of noise reduction technologies for a small direct-injection diesel engine. JSAE Review 2001;21:327–33.

[12] Shi X-Y, Qiao X-Q, Ni J-M, Zheng Y-Y, Ye N-Y. Study on the combustion and emission characteristics of a diesel engine with multi-injection modes based on experimental investigation and computational fluid dynamics modelling. Proc Inst Mech Engrs, J Automobile Engng 2010;224:1161–76.

[13] Benajes J, Novella R, Garcia A, Arthozhoul S. The role of in-cylinder gas density and oxygen concentration on late spray mixing and soot oxidation processes. Energy 2011;36:1599–611.

[14] Torregrosa AJ, Broatch A, Novella R, Monico LF. Suitability analysis of advanced diesel combustion concepts for emissions and noise control. Energy 2011;36:825–38.

[15] Watanabe Y, Fujisaki H, Tsuda T. DI Diesel engine becomes noisier at acceleration – the transient noise characteristic of diesel engine. SAE paper no. 790269, 1979.

[16] Head HE and Wake JD. Noise of diesel engines under transient conditions. SAE paper no. 800404, 1980.

[17] Rust A, Thien GE. Effect of transient conditions on combustion noise of NA-DI diesel engines. SAE paper no. 870989, 1987.

[18] Dhaenens M, van der Linden G, Nehl J, Thiele R. Analysis of transient noise behavior of a truck diesel engine. SAE paper no. 2001-01-1566, 2001.

[19] Watson N, Janota MS. Turbocharging the internal combustion engine. London: MacMillan; 1982.

[20] Alt N, Sonntag H-D, Heuer S, Thiele R. Diesel engine cold start noise improvement. SAE paper no. 2005-01-2490, 2005.

[21] AVL 450 Combustion Noise Meter, Operating Manual, AVL, August 2000.

[22] Soid SN, Zainal ZA. Spray and combustion characterization for internal combustion engines using optical measuring techniques - a review. Energy 2011;36:724–41.

[23] Rakopoulos CD, Mavropoulos GC. Effects of transient diesel engine operation on its cyclic heat transfer: an experimental assessment. Proc Inst Mech Engrs, J Automobile Engng 2009;223:1373–94.

[24] Hagena JR, Filipi ZS, Assanis DN. Transient diesel emissions: analysis of engine operation during a tip-in. SAE paper no. 2006-01-1151, 2006.

[25] Shu G, Wei H. Study of combustion noise mechanism under accelerating operation of a naturally aspirated diesel engine. Int. J. Vehicle Design 2007;45:33–47.

[26] Rakopoulos CD, Giakoumis EG. Review of thermodynamic diesel engine simulation under transient operating conditions. SAE paper no. 2006-01-0884, 2006.

[27] Rakopoulos CD, Dimaratos AM, Giakoumis EG, Rakopoulos DC. Investigating the emissions during acceleration of a turbocharged diesel engine operating with bio-diesel or n-butanol diesel fuel blends. Energy 2010;35:5173–84.

[28] Priede T. Relation between form of cylinder pressure diagram and noise in diesel engines. Proc Inst Mech Engrs 1961;1:63–77.

[29] Strahle WC. Combustion randomness and diesel engine noise: theory and initial experiments. Combustion and Flame 1977;28:279–90.

Table 1

Engine model and type	Mercedes-Benz OM 366 LA, 6 cylinder, in-line, 4-stroke, compression ignition, direct injection, water-cooled, turbocharged, aftercooled, with bowl-in-piston
Speed range	800–2600 rpm
Maximum power	177 kW @ 2600 rpm
Maximum torque	840 Nm @ 1250–1500 rpm
Engine total displacement	5958 cm^3
Bore/Stroke	97.5mm/133 mm
Compression ratio	18:1
Fuel pump	Bosch PE-S series, in-line, 6-cylinder with fuel limiter
Static injection timing	5±1° crank angle before TDC (at full load)
Turbocharger model	Garrett TBP 418-1 with internal waste-gate
Aftercooler	Air-to-Air

Table 2

Parameter	Measuring device	Error
Engine speed	'Kistler' shaft encoder	0.02° CA
Cylinder pressure	'Kistler' miniature piezoelectric transducer, combined with 'Kistler' charge amplifier	< ±1% FSO
Fuel pump rack position	Linear variable differential transducer (LVDT)	0.1 mm
Boost pressure	'Wika' pressure transmitter	< ±1% FSO
Turbocharger speed	'Garrett' turbo speed sensor (including gauge)	± 0.5% FSO
Combustion noise	AVL 450 combustion noise-meter	< ± 1 dBA

Table 3

Test No.	Transient	Initial Conditions		Final Conditions	
		Speed (rpm)	Load (%)	Speed (rpm)	Load (%)
1.	Acceleration	1035	10	1670	12
2.	Acceleration	1035	10	2110	18
3.	Acceleration	1530	10	2080	20
4.	Acceleration	1530	40	2055	75
5.	Acceleration (slow)	1420	30	1845	52
6.	Acceleration (fast)	1420	30	1845	52
7.	Load increase	2034	10	1202	50

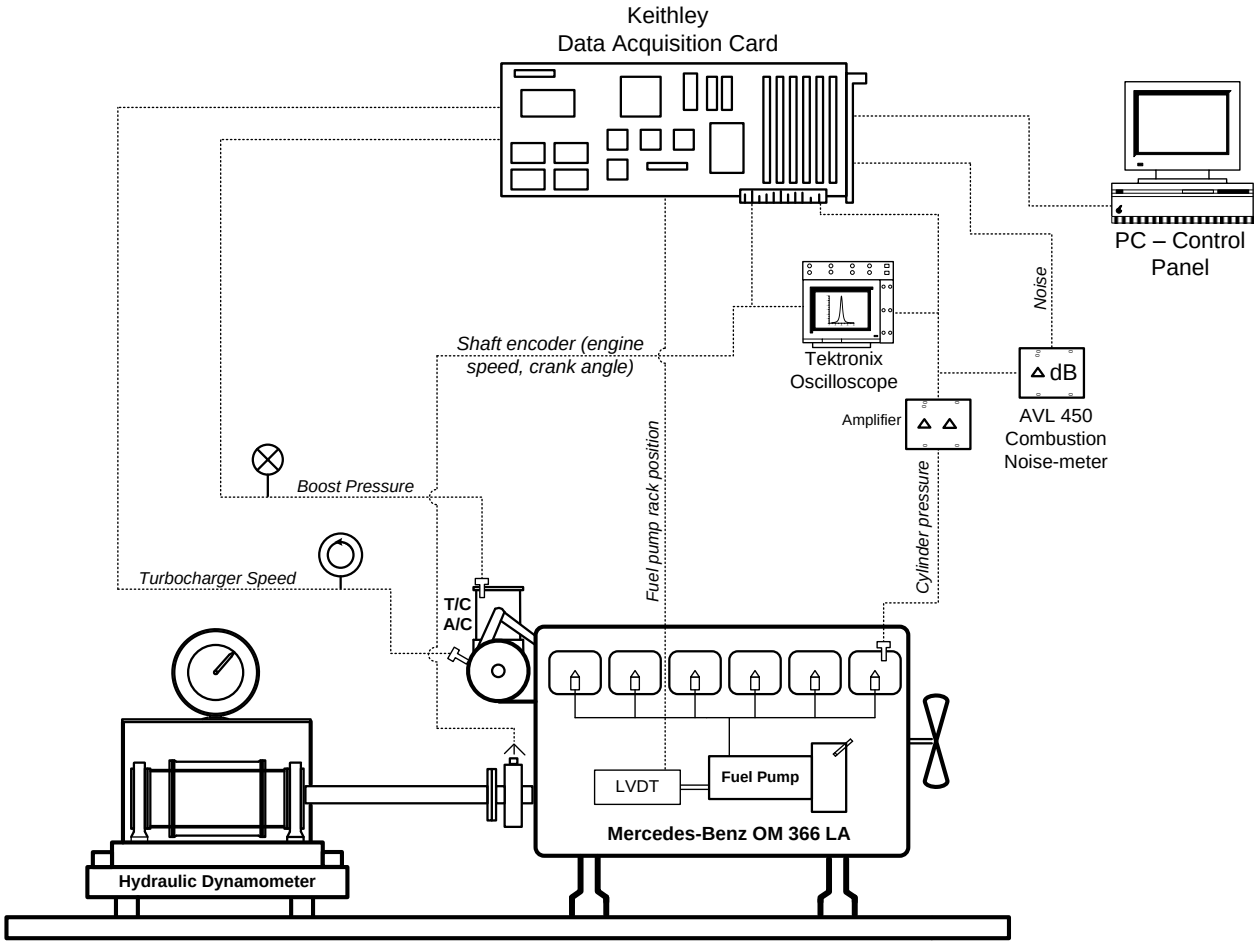

Fig. 1 – Schematic layout of the test bench installation

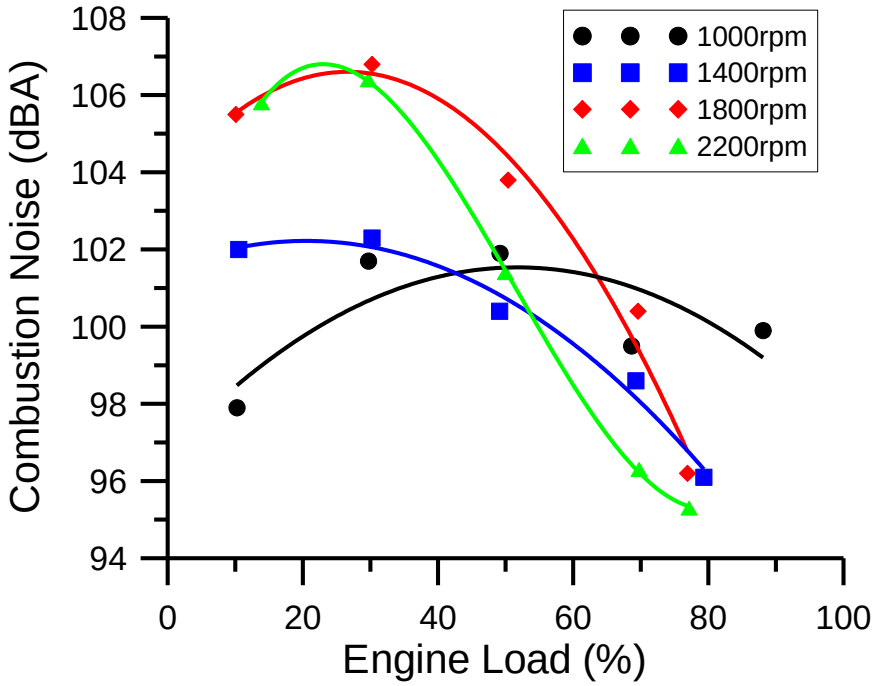

Fig. 2 – Steady-state map of engine combustion noise

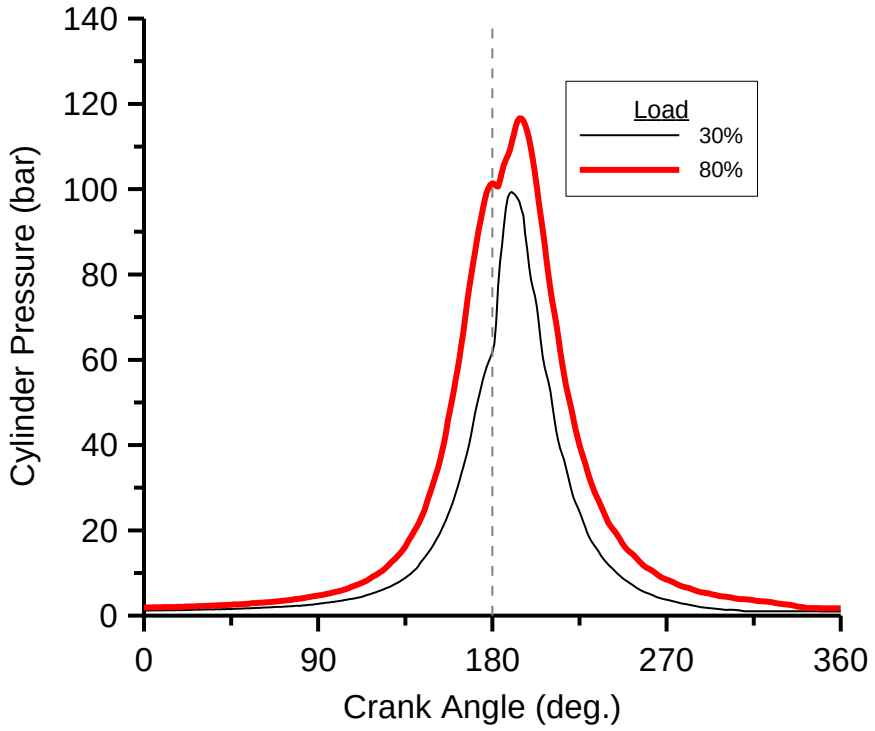

Fig. 3 – Two representative steady-state cylinder pressure diagrams at 1800 rpm

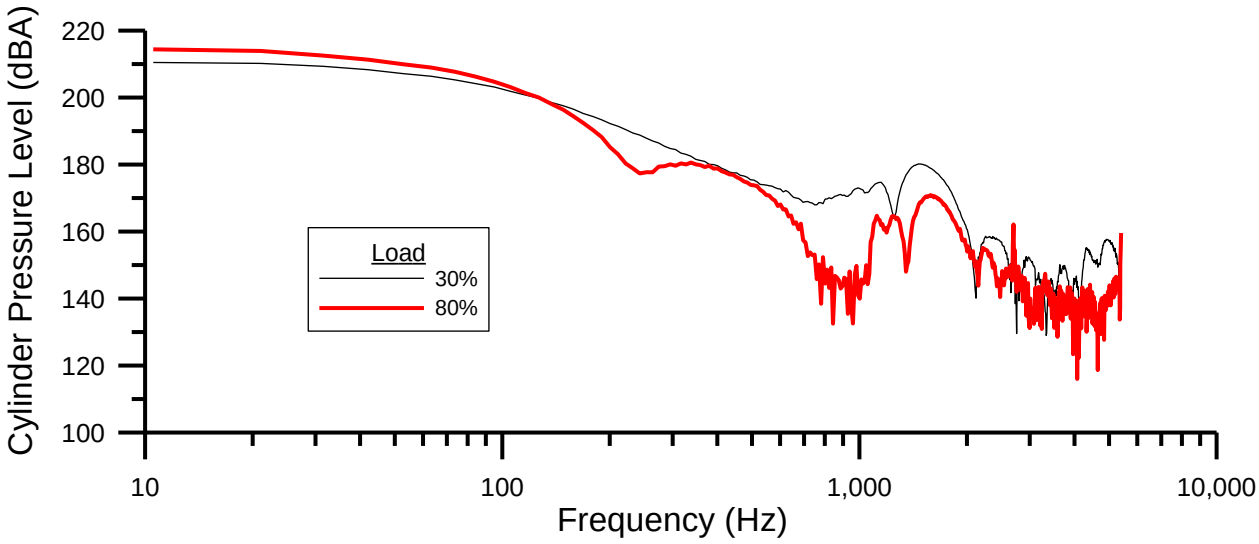

Fig. 4 – Steady-state cylinder pressure level at 1800 rpm for the two loads/indicator diagrams of Fig. 3

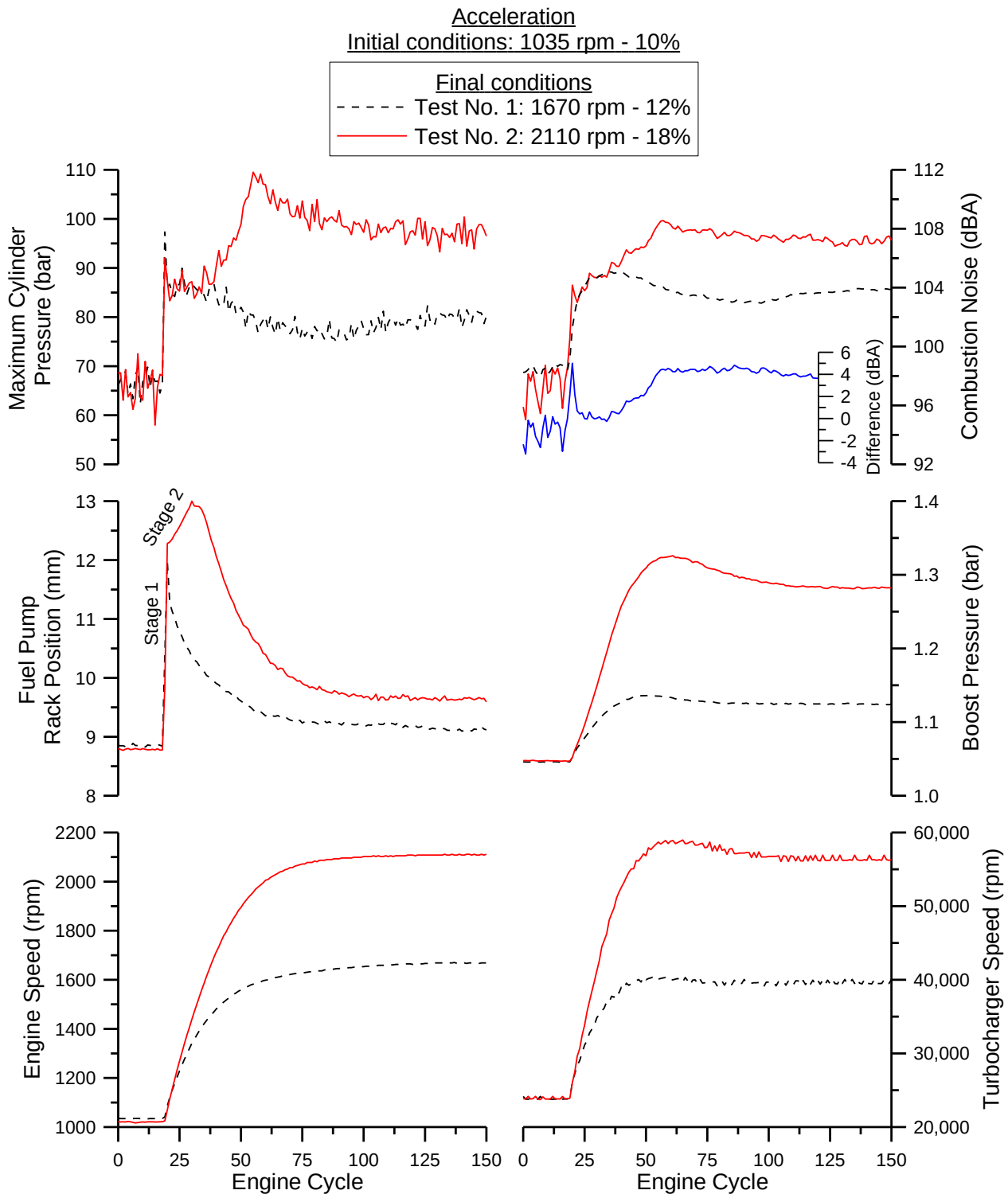

Fig. 5 – Development of engine and turbocharger variables and combustion noise radiation during two accelerations from low load

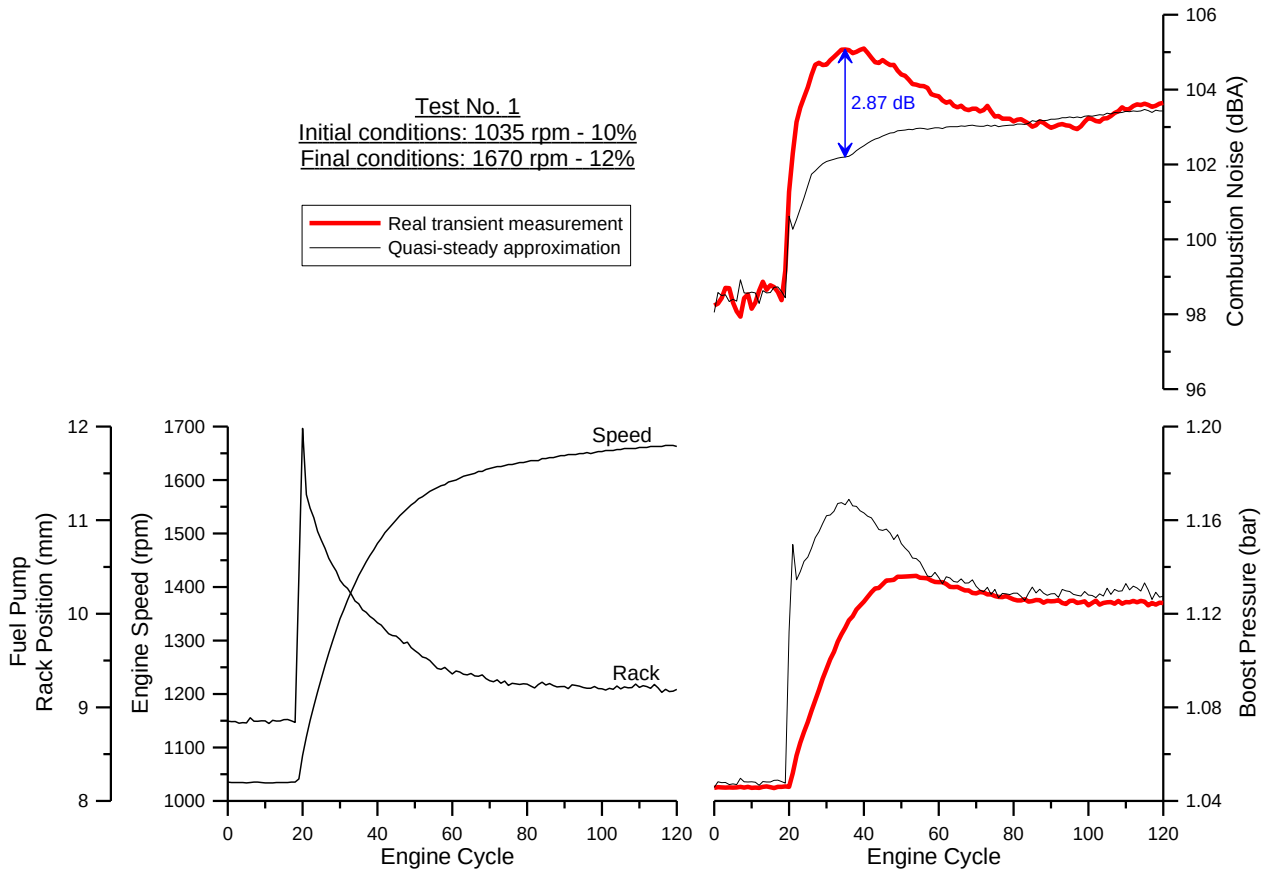

Fig. 6 – Quasi-steady approximation of combustion noise development during acceleration test No. 1, and comparison with actual transient measurements

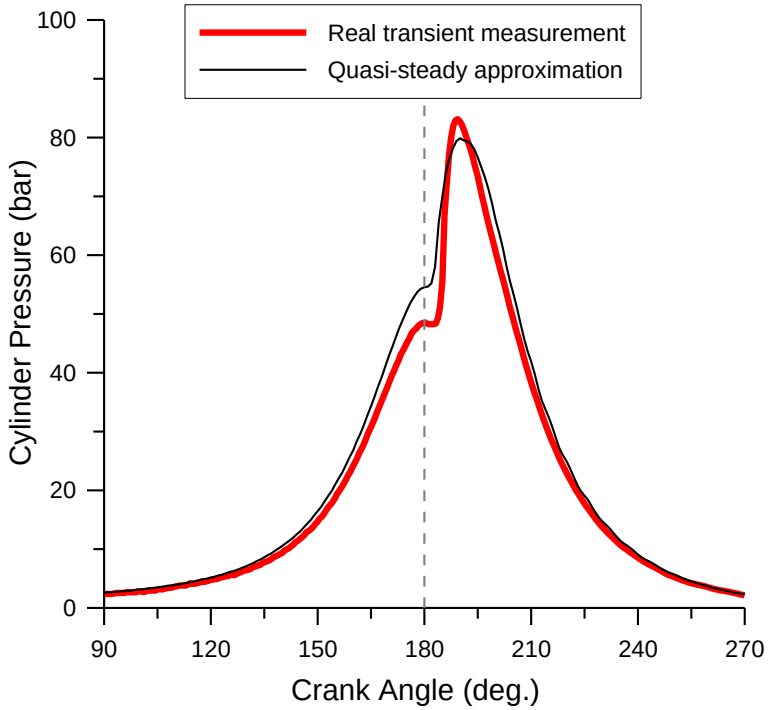

Fig. 7 – Comparison of cylinder pressures for the two cycles exhibiting the higher noise difference during the real transient vs. quasi-steady approximation of Fig. 5

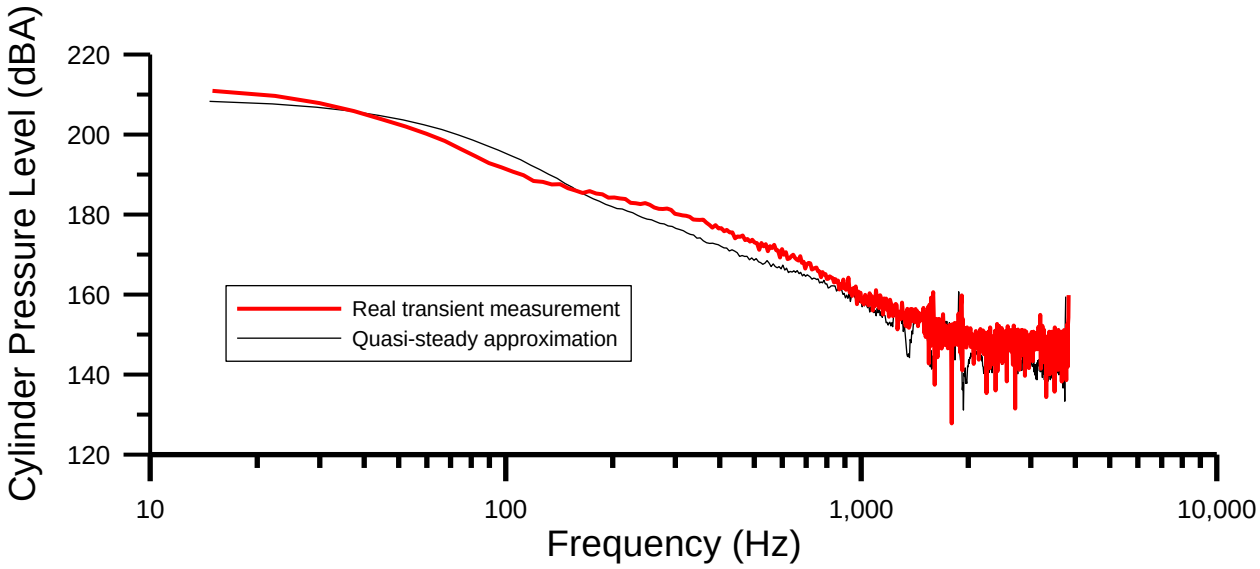

Fig. 8 – Comparison of cylinder pressure level for the two cycles exhibiting the higher noise difference during the real transient vs. quasi-steady approximation of Fig. 5

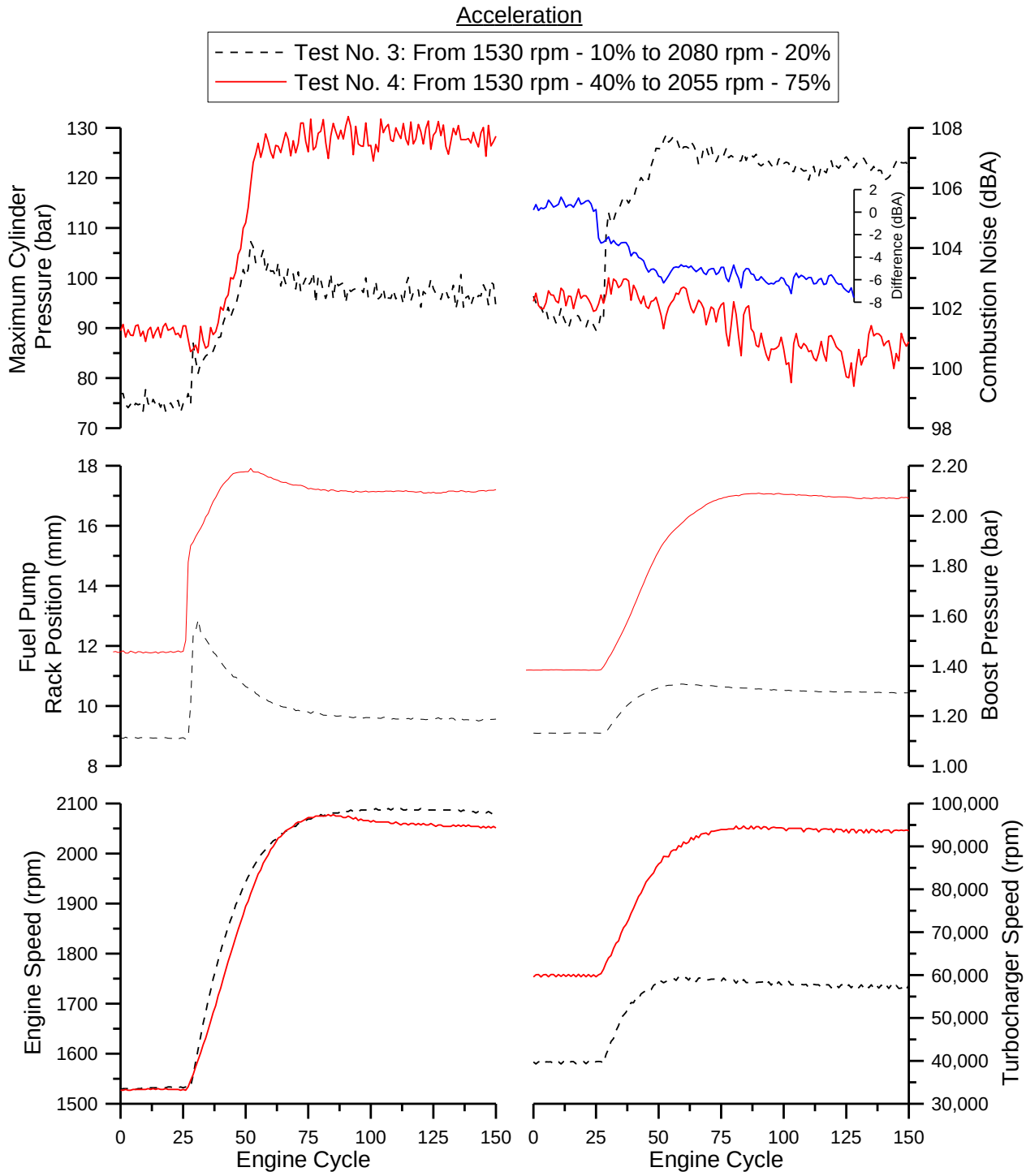

Fig. 9 – Development of engine and turbocharger variables and combustion noise radiation during the acceleration tests No. 3 and 4

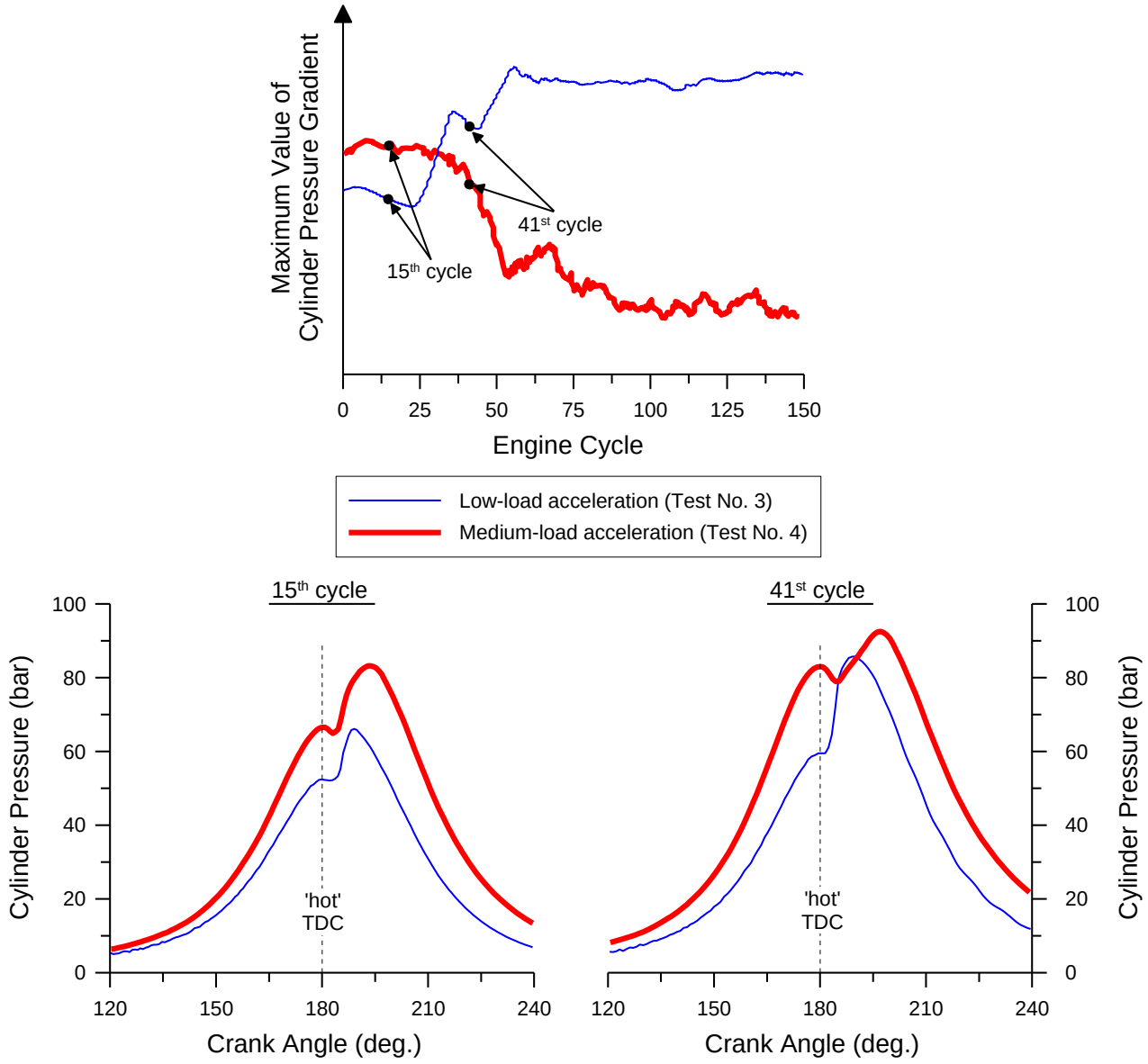

Fig. 10 – Diagrams of cylinder pressure and its first derivative for two selected cycles during the acceleration tests No. 3 and 4

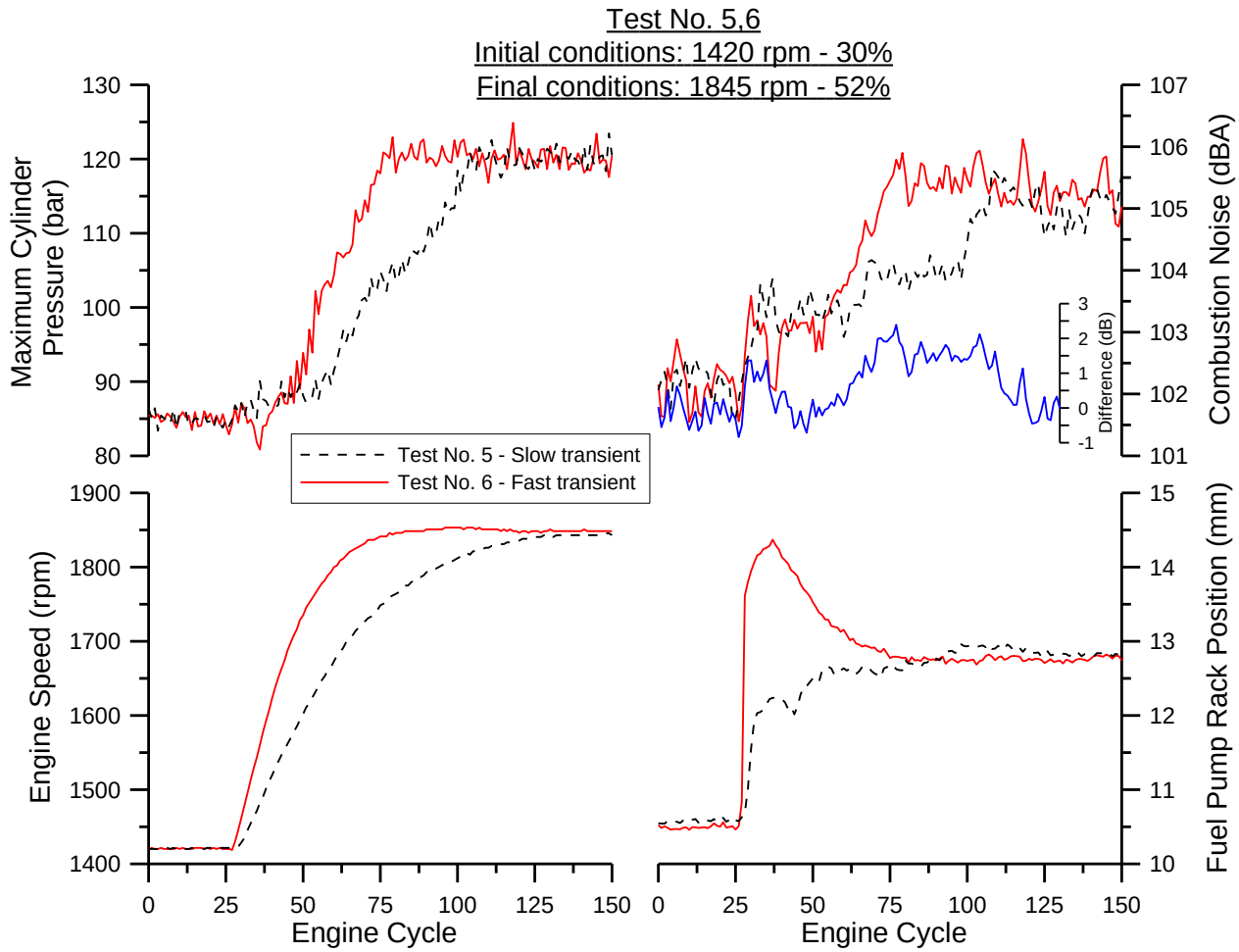

Fig. 11 – Development of engine and turbocharger parameters and combustion noise radiation during an acceleration test conducted at slow and fast rate

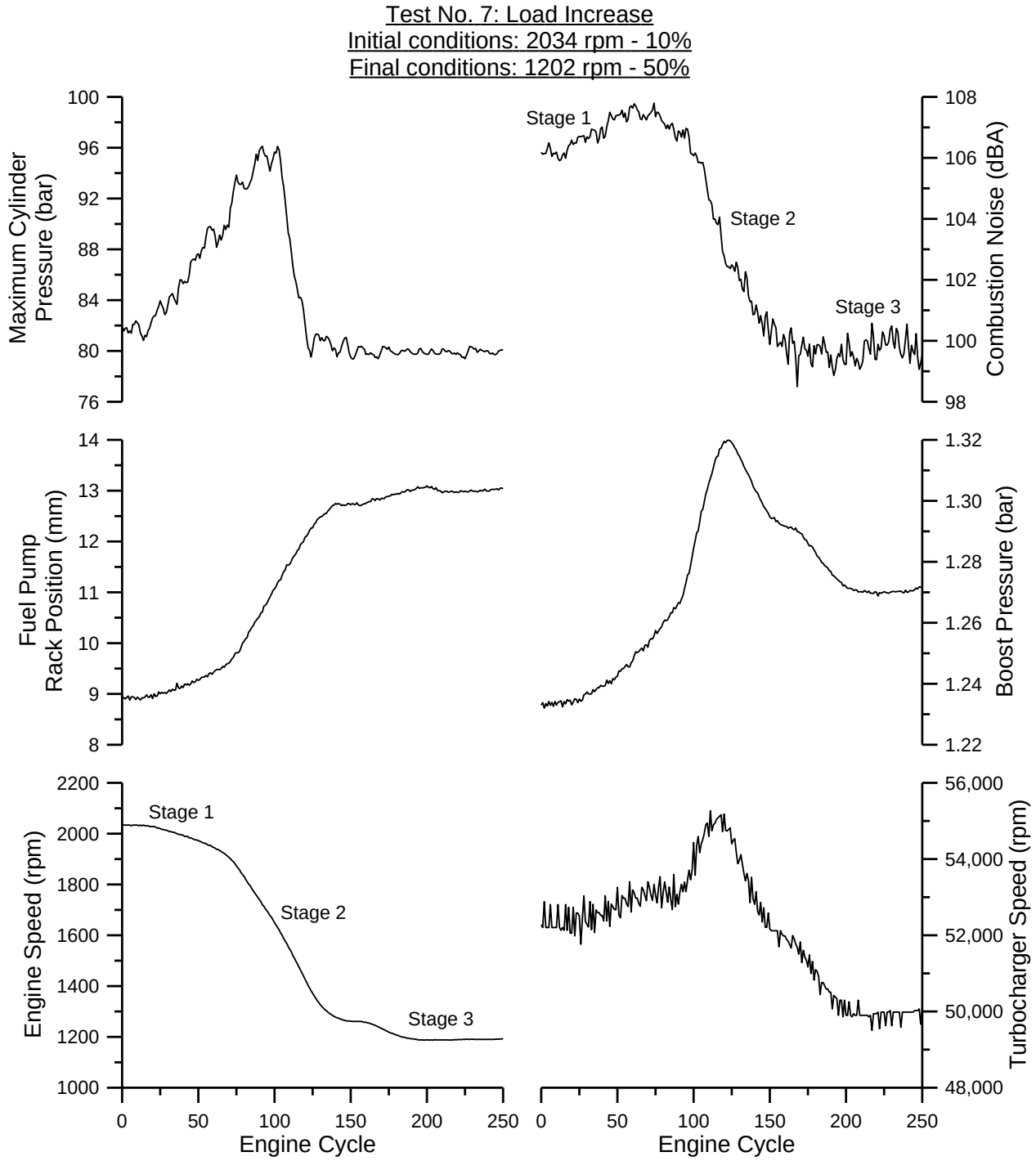

Fig. 12 – Development of engine and turbocharger variables and combustion noise radiation during a load increase transient event

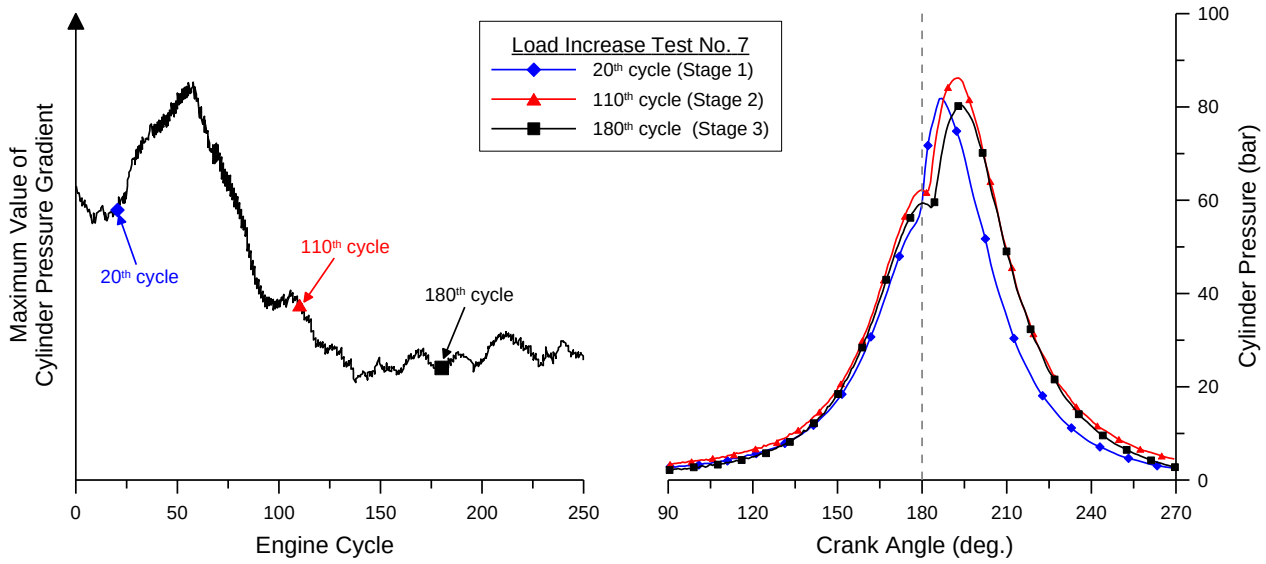

Fig. 13 – Diagrams of cylinder pressure and its first derivative for three selected cycles during the load increase test No. 7 of Fig. 12

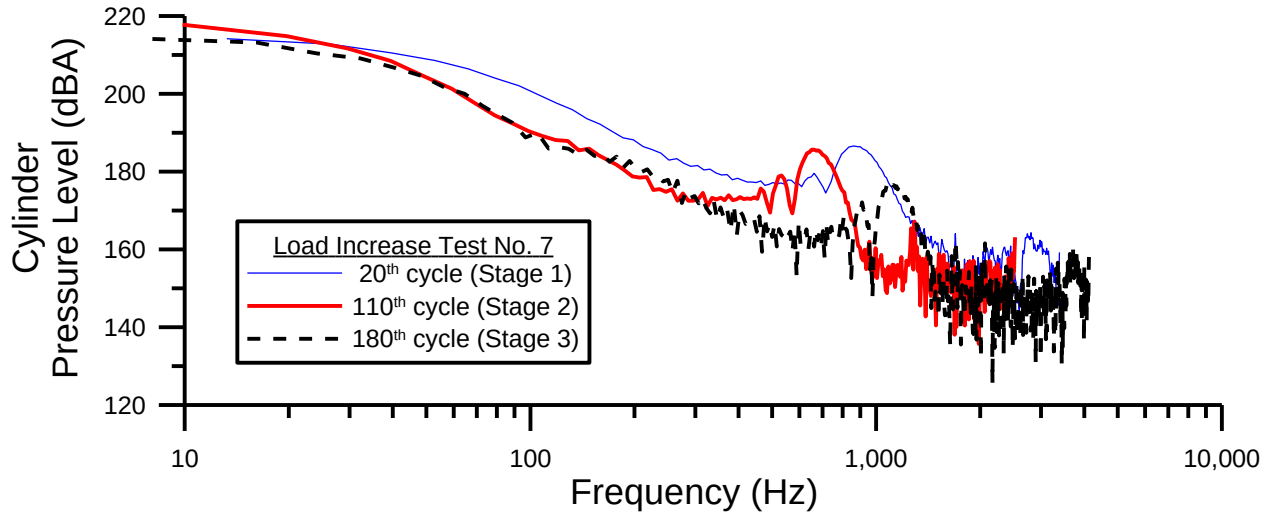

Fig. 14 – Cylinder pressure frequency spectrum for three selected cycles during the load increase test No. 7 of Fig. 12